hexagon, the charges are −0.1467 and −0.0491, respectively, whereas for atoms on opposite sides of the cluster the comparable values are −0.1292 and −0.0942. In both cases the boron is more negative than the nitrogen. The energies of the three isomers of ($@C_{58}BN$) are almost identical, with the B–N bonded structure slightly favored.

III. Conclusion

While we reiterate here the semiquantitative nature of our results, it must nevertheless be stated that MNDO is best suited to our present purpose. Our intention is to compare a large number of different structures where electrons are globally delocalized. This appears to preclude classical calculations, which would not properly account for the delocalization. Assuming that the discrepancy between MNDO and experiment accrues mostly from strain energy, and noting that the strain energy must be approximately constant among all structures studied, MNDO would appear to be the method of choice.

The essential qualitative result may thus be summarized as follows: It seems that BN-substituted derivatives of ($@C_{60}$) will be stable, especially those species which are isoelectronic with bucky ball. From the reactions described by eqs 2a–c, it seems that ($@C_{12}B_{24}N_{24}$) is more stable than bucky ball, which is slightly more stable than ($@B_{30}N_{30}$). The significantly lower reaction enthalpy for the formation of CBN-ball is due in part to the relative instability of the naphthalene-like precursor. But, based on total energies (Table II), all species rival bucky ball with respect to thermodynamic stability.

Kinetic stability is harder to judge. As was noted above, bucky ball has been synthesized by the pyrolysis of benzene.[13] This suggests that ($@B_{30}N_{30}$) might be obtained from borazine either by thermal degradation as per eq 1b or by high-temperature air

oxidation.[19]   ($@C_{12}B_{24}N_{24}$) represents a more difficult synthetic problem. Precursors having C:B:N atomic ratios of 1:2:2 would be especially attractive, as illustrated by eq 2c, but such species are rare. However, a synthetic route to compounds having fused CB_2N_2 rings has been described.[12]

Once made, both BN-ball and CBN-ball are expected to have significantly different chemical properties from those of ($@C_{60}$). Bucky ball itself is reactive toward both nucleophiles and electrophiles.[20]   The uneven charge distributions of the B– and N-doped clusters should increase both types of reactivity, making them attractive as ligands, electron transfer agents, etc. They would be important additions to the chemical arsenal.

(19) A detailed study has been carried out on the formation of ($@C_{60}$) by high-temperature air oxidation. See: Saxby, J. D.; Chatfield, S. P.; Palmisano, A. J.; Vassallo, A. M.; Wilson, M. A.; Pang, L. S. K. *J. Phys. Chem.*, submitted.

(20) For reviews, see: Diederich, F.; Whetten, R. L. *Angew. Chem., Int. Ed. Engl.* **1991**, *30*, 678. Wudl, F.; Hirsch, A.; Khemani, K. C.; Suzuki, T.; Allemand, P.-M.; Koch, A.; Srdanov, G. *Abstracts of Papers*, A.C.S. Symposium on Large Carbon Clusters; American Chemical Society: Washington, DC, 1991.

Momentum Distributions, Spin Distributions, and Bonding in CH₃NH₂ and Its Radical Cation

Christopher J. Maxwell, Francisco B. C. Machado, and Ernest R. Davidson*

Contribution from the Chemistry Department, Indiana University, Bloomington, Indiana 47405. Received February 13, 1992

Abstract: Theoretical spherically averaged momentum distributions for canonical Hartree–Fock and Dyson orbitals are presented for methylamine and compared with the EMS spectra. Theoretical spin densities are also reported for the radical cation and compared with the EPR spectrum. To the first approximation, both of these experiments give information about the HOMO of the neutral molecule. Both results clearly show effects from hyperconjugative delocalization of the nitrogen lone-pair onto the methyl group. The methyl group is found to be electron withdrawing relative to hydrogen in forming methylamine from ammonia. The amino group is similarly electron withdrawing relative to hydrogen in forming methylamine from methane.

Introduction

Data from electron momentum spectroscopy[1,2] and electron paramagnetic resonance spectroscopy[3] are available for methylamine and its radical cation. These results and previous theory[1,2,4–6]

for this molecule are interpreted on the basis of new calculations.

Electron momentum spectroscopy[7] (EMS), also known as (e,2e) spectroscopy, has recently proven to be a very effective probe of electronic structure. Experimentally, an electron beam of high energy is directed at gas-phase target molecules, resulting in a scattered electron, an ejected electron, and a molecular cation. The few pairs of outgoing electrons which happen to have equal energies and both paths at an angle θ (usually 45°) to the unscattered beam are selected for detection. The azimuthal angle ϕ between the planes defined by the incoming and outgoing

(1) Tossell, J. A.; Lederman, S. M.; Moore, J. M.; Coplan, M. A.; Chornay, D. J. *J. Am. Chem. Soc.* **1984**, *106*, 976. Tossell, J. A.; Moore, J. H.; Coplan, M. A. *Int. J. Quantum Chem.* **1984**, *S18*, 483.
(2) Bawagan, A. O.; Brion, C. E. *Chem. Phys.* **1988**, *123*, 51.
(3) Knight, L. B. Private communication.
(4) Hehre, W. J.; Pople, J. A. *Tetrahedron Lett.* **1970**, *34*, 2959.
(5) Umeyama, H.; Morokuma, K. *J. Am. Chem. Soc.* **1976**, *98*, 4400.
(6) Murray, J. S.; Politzer, P. *Chem. Phys. Lett.* **1988**, *152*, 364.

(7) See for example: Duffy, P.; Casida, M. E.; Brion, C. E.; Chong, D. P. *Chem. Phys.* **1992**, *159*, 347 and references therein.

Momentum and Spin Distributions and Bonding in CH$_3$NH$_2$

J. Am. Chem. Soc., Vol. 114, No. 16, 1992 6497

electron beams is then the only remaining variable. The initial momentum, **p**, of the target electron (before ionization) is determined from

$$\mathbf{p} + \mathbf{p}_0 = \mathbf{p}_1 + \mathbf{p}_2 \tag{1}$$

where $\mathbf{p}_0$ is the momentum of the incoming electron and $\mathbf{p}_1$ and $\mathbf{p}_2$ are the outgoing momenta. This equation assumes the change in momentum between the target molecule and the ion is simply $-\mathbf{p}$. Under the experimental conditions, this gives a simple equation for the magnitude of the initial momentum

$$p^2 = (2p_1 \cos\theta - p_0)^2 + (2p_1 \sin\theta \cos(\tfrac{1}{2}\phi))^2 \tag{2}$$

Theoretical calculations describing this process may be carried out by applying the plane wave impulse approximation. The estimated cross section, σ, for the (e,2e) process is proportional to

$$\sigma \propto g_f \int d\Omega_p/4\pi \, |\langle p\Psi_f^{N-1}|\Psi_0^N\rangle|^2 \tag{3}$$

where p represents a momentum eigenfunction for one electron. The wave functions denote the initial neutral and final ionic states, resulting in the ion–neutral overlap distribution (OVD). The integral over Ω_p indicates spherical averaging over momentum directions and is equivalent to rotational averaging over target molecule positions. By varying the energy of the incoming electron beam, with fixed outgoing energy, the cross section for various final ion states can be detected. The factor g_f is the degeneracy of the final state.

One can simplify this equation considerably by utilizing the Hartree–Fock ground state for the neutral molecule wave function and representing the ion state by the initial state with the orbital of interest removed (Koopmans' approximation). The above equation then simplifies to

$$\sigma \propto g_f \int d\Omega_p/4\pi \, |\psi(\mathbf{p})|^2 \tag{4}$$

with ψ as the momentum space representation of the canonical Hartree–Fock molecular orbital from which the electron was ionized.

If better wave functions are used to represent these states, the OVD after renormalization has the form of a Dyson orbital

$$\psi = S^{-1}\langle \Psi_f^{N-1}|\Psi_0^N\rangle_{N-1} \tag{5}$$

where the subscript on the bracket is a reminder that integration is only done over $N-1$ electrons and S is the normalization constant. The cross section is then given by

$$\sigma \propto S^2 g_f \int d\Omega_p/4\pi \, |\psi(\mathbf{p})|^2 \tag{6}$$

where S^2 is now the "pole-strength". It is usually found that ion states may be classified as "primary hole states" where S is near unity and "satellite states" where S is small. The satellite states are excited states of the ion in which, to the first approximation, one electron has been excited into a virtual orbital in addition to one being ionized. In almost all cases, including satellite states, the normalized Dyson orbital gives a cross section indistinguishable within experimental error from one of the Koopmans orbitals.

Electron paramagnetic resonance (EPR) is a method for learning about the molecular orbital which contains the unpaired electron in a radical. The EPR data may be summarized in the isotropic and anisotropic hyperfine coupling constants describing the interaction between electron and nuclear spin. For the exact wave function of the ground state of the ion, Ψ_0^{N-1}, these parameters can be computed from the unpaired spin density[8]

$$\rho_s \, (\rho_\alpha - \rho_\beta)/(N_\alpha - N_\beta) \tag{7}$$

where ρ_α and ρ_β are the density of electrons with spin up or spin down. The hyperfine constants are given by

$$A_{iso} = (8\pi g_e g_n \beta_n/3g_0)\rho_s(\mathbf{R}_n)$$

$$A_{aniso}(i,j) = -(g_e g_n \beta_n/g_0) \int \rho_s Q_{ij} \, d\tau \tag{8}$$

$$Q_{ij} = (3r_i r_j - r^2\delta_{ij})/r^5$$

where r_i is one of the x, y, z components of $\mathbf{r}$ and $\mathbf{R}_n$ is the nuclear position. A_{iso} is a measure of the Fermi contact interaction while A_{aniso} measures the dipolar spin–spin interaction.

If the wave function for the ground state of the ion is approximated by a spin restricted Slater determinant then the spin density is just the square of the highest occupied molecular orbital (HOMO). In this approximation, the values of A_{iso} sample the HOMO density at the nuclei. In Koopmans' approximation, this half-occupied HOMO is the same orbital that is half-emptied in the EMS experiment for the lowest state of the ion. Hence both experiments are giving information about the same orbital which, for methylamine, is the nitrogen lone pair. Of course, with better wave functions this equivalence disappears.

Another problem in this comparison is that the EMS data are not vibrationally resolved and are best approximated by using the nuclear conformation at the neutral molecule equilibrium geometry. The EPR data, on the other hand, are for the cold ion and are best approximated using the ion geometry. For rigid molecules this would not matter, but for methylamine there may be significant repyramidalization at the nitrogen when a lone-pair electron is removed. The isoelectronic ethyl radical has been widely studied by EPR and theory. It is known to be a rather floppy molecule for which theory gives a wide variety of conformations.[9] The barrier for internal rotation is <1 kJ/mol, and this rotation is strongly coupled to flapping motion at the methylene carbon.

In this paper we compare EPR and EMS data with calculated properties for NH$_3$, CH$_4$, and CH$_3$NH$_2$. The EMS data have previously been interpreted as showing electron withdrawal by the methyl groups in the sequence NH$_{3-p}$(CH$_3$)$_p$, $p = 0, 1, 2, 3$, although actually only electron transfer in the HOMO of the neutral molecule is shown by the data.[2] Certainly the EPR data agree that the HOMO of the cation is delocalized onto the methyl hydrogens.[3] Although these conclusions support each other, experiments of these two types have not been compared in the chemical literature.

Hehre and Pople[4] have pointed out that the methyl group in neutral methylamine is electron withdrawing relative to one of the hydrogens in ammonia. As such, all the orbitals are involved and the net effect cannot be judged from the HOMO alone. Since carbon is more electronegative than hydrogen, it should be relatively less donating to nitrogen. Hence it would appear to be electron withdrawing on a scale where hydrogen is chosen as the reference "zero". This argument, however, applies to the CN σ bond and not to the nonbonding electrons.

The zeroth order approximation for nonbonding electrons is that the occupied orbitals of the fragments will mix to form delocalized orthonormal orbitals of the molecule, but this will not result in any net charge transfer. That is, if π_{CH} and n_N are non-orthogonal MO's localized on the fragments,[10] the wave function formed from doubly occupying both of the orthonormal MO's (a π_{CH} + b n_N) and (−b′ π_{CH} + a′ n_N) is identical to the wave function with π_{CH} and n_N doubly occupied. Additionally there may be an anomeric effect from mixing with the π_{CH}* orbital that will result in some charge transfer.

The EPR data, on the other hand, are conventionally explained as a hyperconjugation effect in the radical. Methylamine radical cation nominally has a spin-up electron in the nitrogen lone-pair orbital and an electron pair in a CH bond orbital that makes a 180° dihedral angle with the axis of the nitrogen lone-pair orbital. The spin-down electron of the CH bond delocalizes into the hole in the lone-pair orbital and stabilizes the radical by forming the best possible MO of the form (a π_{CH} + b n_N). The wave function

(8) See for example: Feller, D.; Davidson, E. R. In *Theoretical Models of Chemical Bonding, Part 3*; Maksic, Z. B., Ed.; Springer-Verlag: Heidelberg, 1991; pp 429–455 and references therein.

(9) See for example: Suter, H. U.; Ha, T. K. *Chem. Phys.* **1991**, *154*, 227 and references therein.

(10) π_{CH} is the e_1 symmetry linear combination of CH σ bonds of the form $2\sigma_1-\sigma_2-\sigma_3$ where σ_1 is the CH bond in the plane of the nitrogen lone-pair orbital.

Table I. Optimized Geometries

molecule		atomic coordinates (bohrs)		
		X	Y	Z
NH_3	H	0	0.735984	0
	N	0	0	1.764086
	H	±1.527743	0.735984	2.646129
NH_3^+	H	0	0	0
	N	0	0	1.928087
	H	±1.669773	0	2.892131
CH_3NH_2	C	0	0	0
	H	0	1.868251	−0.888306
	H	±1.655815	−1.016450	−0.667920
	N	0	0	2.760323
	H	±1.526205	0.959188	3.400156
$CH_3NH_2^+$	C	0	0	0
stagger	H	0	1.990321	−0.599019
	H	±1.708691	−0.891764	−0.696567
	N	0	0	2.700607
	H	±1.637899	0.056624	3.711614
$CH_3NH_2^+$	C	0	0	0
eclipse	H	1.914966	0	−0.710957
	H	−1.050424	±1.661333	−0.638104
	N	0	0	2.702282
	H	1.626770	0	3.732252
	H	−1.649537	0	3.696334

for the molecule is unchanged by mixing of the spin-up CH and lone-pair orbitals. Hence a ROHF wave function can choose one spin-up orbital to be identical to the delocalized spin-down orbital. The square of the orthogonal antibonding spin-up orbital then gives the spin density.

These two pictures are coupled through Koopmans' theorem. Although the neutral molecule SCF wave function and energy are actually independent of mixing among the occupied orbitals, the usual (so-called "canonical") Hartree–Fock molecular orbitals of the neutral give a unique best choice for describing the radical cation as a hole in an MO of the neutral molecule. Thus the Hartree–Fock equations for the neutral cause a premixing of the MO's so that the removal of an electron from the HOMO gives a good description of the radical cation. Hence the hyperconjugative mixing of the CH bond and nitrogen lone-pair already happens in the neutral molecule and can be detected by EMS as well as EPR spectroscopy. The canonical HOMO orbital of the neutral maximizes the orbital energy (compared to all other ways to mix the occupied orbitals with each other).[11] By Koopmans' theorem, this minimizes the computed ionization energy, and hence minimizes the computed energy of the ion. This is reversed from the usual view that hyperconjugation lowers the orbital energy of the highest spin-down orbital of the ion (which does not correspond to the HOMO of the neutral).

Method

Both Hartree–Fock and configuration interaction calculations (SCF and CI) were performed at the appropriate geometries to provide the basis for the momentum distribution and properties calculations.

Geometry optimizations using GAUSSIAN 86[12] with 6-31G** basis sets at the unrestricted Hartree–Fock second-order Møller–Plesset perturbation theory (UMP2) level were done for all molecules of interest (NH_3, CH_3NH_2, NH_3^+, and $CH_3NH_2^+$). In all subsequent computations the MELD[13] programs were used. Experimental geometries are not well-known for the ionic species, so to keep the results directly comparable computed geometries were used for all four molecules. All the geometries determined can be found in Table I.

(11) This fact follows from the theorem that the highest eigenvalue of a matrix (such as the Fock matrix) gives the maximum average value. Canonical orbitals leave the Fock matrix diagonal. Any other choice of mixing the occupied orbitals would give a lower (i.e. more negative) average value of the Fock matrix for the HOMO.

(12) GAUSSIAN 86: Frisch, M. J.; Binkley, J. S.; Schlegel, H. B.; Raghavachari, K.; Melius, C. F.; Martin, R. L.; Stewart, J. J. P.; Bobrowicz, F. W.; Rohlfing, C. M.; Kahn, L. R.; Defrees, D. J.; Seeger, R.; Whiteside, R. A.; Fox, D. J.; Fleuder, E. M.; Pople, J. A. Carnegie-Mellon Quantum Chemistry Publishing Unit: Pittsburgh, PA, 1984.

(13) The MELDF collection of electronic structure codes was developed by L. E. McMurchie, S. T. Elbert, S. R. Langhoff, and E. R. Davidson and was extensively modified by D. Feller and D. C. Rawlings.
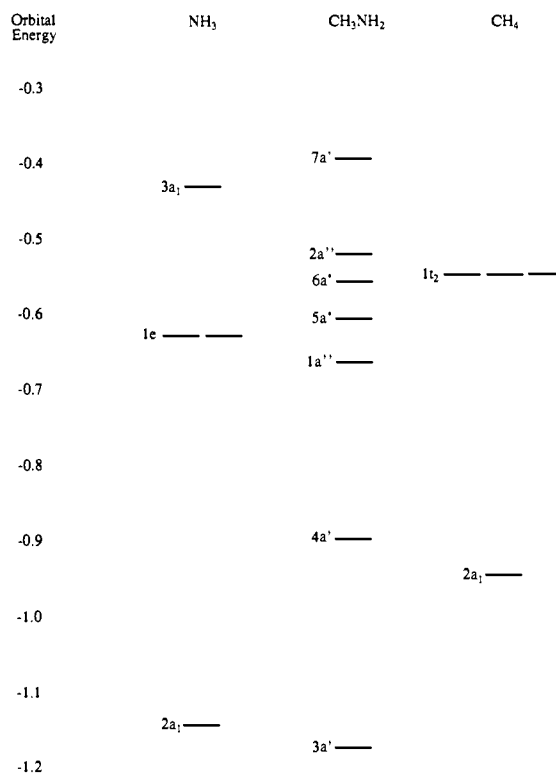
Figure 1. Orbital energies in hartree atomic units.

The $CH_3NH_2^+$ ion has two possible C_s structures. Optimization without symmetry constraints yielded one structure with a CH bond in the same plane with the N lone-pair orbital. Symmetry-constrained optimization yielded a second structure at a slightly higher energy with one CH bond orthogonal to the lone-pair orbital and the CNH_2 group exactly planar. This structure is probably the transition state for internal rotation of the methyl group. We will follow the notation for ethane and refer to the ion with a CH bond in the plane with the lone-pair as "staggered" and the structure with one CH orthogonal to the C–N-lone-pair plane as "eclipsed". Notice that in this notation one CH bond exactly eclipses one NH bond in the "eclipsed" structure. In the neutral structure the NH_2 is strongly pyramidalized with an ethane-like staggered conformation. Like ethane, the eclipsed form has a slightly higher energy and remains pyramidal. The staggered conformation of the radical cation has a nearly planar NH_2 group, but it is still slightly bent in the same direction as the neutral.

Past calculations for EMS cross sections have shown that the results are very sensitive to the long-range tail of the wave function. This is especially so for lone-pair orbitals whose tails are much more diffuse than allowed by conventional basis sets.[14] The calculations in refs 1 and 2 using 4-31G and 4-31G* were qualitatively correct, but quantitatively wrong at low momentum because of this effect. Also, the ESR hyperfine results require accurate representation of orbitals near the nucleus. Small basis sets of the 6-31G** type are not adequate to describe these properties.

The primitive basis for N and C were chosen to be the 18s, 13p Partridge basis sets.[9] Partridge's 10s basis was used for H. The tightest 14 s functions were contracted into 2 s functions using the atomic orbital coefficients for the 1s and 2s orbitals. Similarly, the tightest 7 p functions were contracted into 1 p function using the 2p atomic orbital coefficients. For hydrogen, the tightest 6 s functions were contracted into 1 s function using the 1s atomic orbital coefficients. The rest of the functions were left uncontracted. This scheme lost less than 0.1 kcal/mol in trial SCF calculations on N_2, CO, and CH_4. Polarization functions were optimized for these test molecules and gave (0.490, 1.115) for the N double d Gaussian exponents (dropping the s component of the Cartesian d functions) and (0.361, 1.261) for C. A single p function exponent of 1.30 was found for H. With these functions, the energies were within 3 kcal/mol of the numerical Hartree–Fock limit for N_2 and CO.

(14) Bawagan, A. O.; Brion, C. E.; Davidson, E. R.; Feller, D. *Chem. Phys.* **1987**, *113*, 119.

(15) Partridge, H. *Near Hartree–Fock Quality GTO Basis Sets for the First and Third Row Atoms*, NASA Technical Memorandum 101044, 1989; pp 73 and 79. Partridge, H. *Near Hartree–Fock Quality GTO Basis Sets for the Second Row Atoms*, NASA Technical Memorandum 89449, 1987; p 73.

Table II. Hartree–Fock and CI Results

molecule	state	S^2	energy (au)		ionization potentials (ev)		
			SCF	CI	SCF	CI	exp[e]
NH_3[a]	ground		−56.2220	−56.4518			
	$(3a)^{-1}$	0.87		−56.0593	11.7	10.7	10.9
	$(1e)^{-1}$	0.87		−55.8489	17.1	16.4	16.5
	$(2a)^{-1}$	0.39		−55.4554	31.1	27.1	
CH_3NH_2[a]	ground		−95.2589	−95.6127			
	$(7a')^{-1}$	0.84		−95.2537	10.7	9.8	9.6
	$(2a'')^{-1}$	0.84		−95.1134	14.1	13.6	13.2
NH_3^{+}[a]	$(3a)^{-1}$		−55.8724	−56.0611	9.5	10.6	10.9
$CH_3NH_2^{+}$[a]	$(7a')^{-1}$		−94.9450	−95.2689	8.5	9.4	9.6
NH_3^{+}[b]	$(3a)^{-1}$	1	−55.9010	−56.0918	8.7	9.8	
$CH_3NH_2^{+}$[c]	$(7a')^{-1}$		−94.9717	−95.2980	7.8	8.6	
$CH_3NH_2^{+}$[d]	$(7a')^{-1}$		−94.9717	−95.2952			

[a] Neutral molecule optimized geometry. [b] NH_3^{+} optimized geometry. [c] $CH_3NH_2^{+}$ optimized staggered geometry. [d] $CH_3NH_2^{+}$ optimized eclipsed geometry. [e] Reference 13.

In the discussion to follow, the orbital labels given in the text refer to the actual point group of the molecule even though MELD routines can only handle subgroups of D_{2h}. For example, even though NH_3^{+} has D_{3h} symmetry the calculation was done imposing C_s symmetry. Figure 1 gives the orbital energies for the neutral molecules of interest. Table II gives the SCF energies and the ionization energies computed from Koopmans' theorem (listed on the line with the neutral molecule) and from the difference in RHF energies (listed on the line with the ion energy).

In order to account for electron correlation, multireference singles and doubles configuration interaction (MRSDCI) computations were done for some of the states. To choose the reference configurations to include in the MRSDCI, we first performed a Hartree–Fock SDCI using perturbation theory to select the important states. K orbitals with frozen core electrons were utilized for all CI calculations. For NH_3 at the optimum geometry, an estimated 75% of the valence shell correlation energy was recovered, and 66% was accounted for in CH_3NH_2. Table II gives the CI ionization energies calculated by using the neutral molecule orbitals for both states and also ion restricted open-shell Hartree–Fock (ROHF) orbitals for the ion. Either method gives ionization energies close to the experimental value.

Momentum distribution plots were generated at both the Koopmans' theorem and CI level of calculation for the outer valence orbitals of ammonia and methylamine from the equation

$$\rho(p) = \int d\Omega_p/4\pi \ |\psi(\mathbf{p})|^2 \qquad (9)$$

Neither the pole strength nor the degeneracy factor have been included. The plots are in general agreement with ref 1 except that they included the factor $g_f = 2$ in their plots. In addition, Koopmans' orbital momentum plots were computed for the valence orbitals of methane and the inner valence orbitals of methylamine to assist in the discussion of the orbital character of these three species. The hyperfine coupling constants were evaluated for the lowest energy state of the ion at the neutral geometry with use of Koopmans' theorem and ROHF and CI wave functions. They also were reevaluated at the relaxed ion conformation. For comparison, Mulliken populations were computed for several wave functions.

Results

The spherical average of the square of the orbital in momentum space is shown in Figures 2 and 3 for the valence orbitals of CH_4. Plots showing significant density at large momentum can be interpreted as having a wave function that varies more rapidly (i.e., with shorter wavelength) in position space. Functions of p or d character transform into p or d functions in momentum space and are all mapped to the origin regardless of their origin in position space. The spherical average of the square of an atomic orbital, which occurs in the EMS intensity, has a contribution that goes like k^{2L} where L is the angular momentum. Symmetry-imposed nodal character in a molecular orbital also produces nodes in momentum space and causes a zero value that behaves like k^{2p} near zero momentum (where p is the number of intersecting nodal surfaces). The density at zero momentum can be written as

$$\rho(0) = |\int d\tau \ \psi(\mathbf{r})|^2 \qquad (10)$$

and is due only to the presence of s orbitals from various atomic centers adding with the same sign. The t_2 orbital of methane is
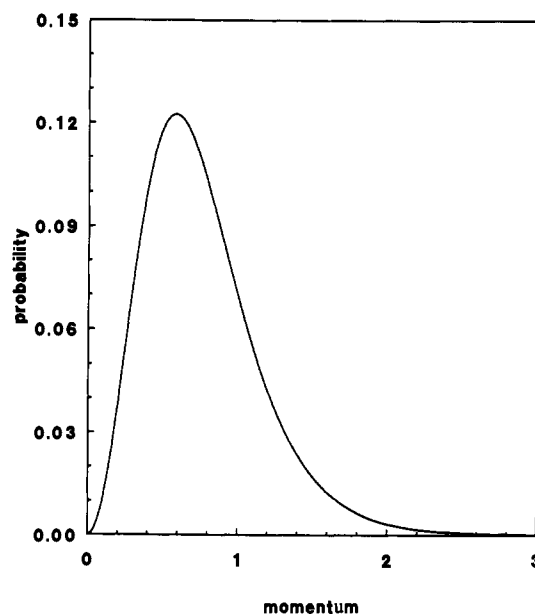
Figure 2. Spherically-averaged momentum density for the $1t_2$ orbital of CH_4. Momentum is given in units of $\hbar/a_0$ and probability density is given in units of $(a_0/\hbar)^3$. See eq 9.
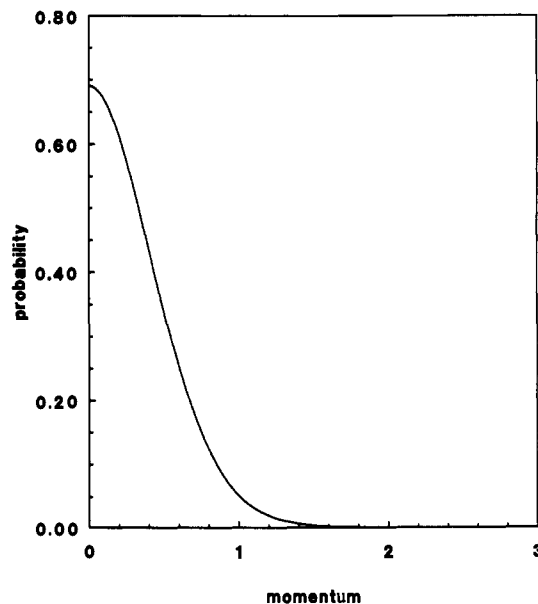
Figure 3. Spherically-averaged momentum density of the 2a orbital of CH_4.

composed almost equally of p orbitals from carbon and a t_2 combination of s orbitals from hydrogen. This gives a probability that is zero at zero momentum. The $2a_1$ orbital of CH_4 is com-
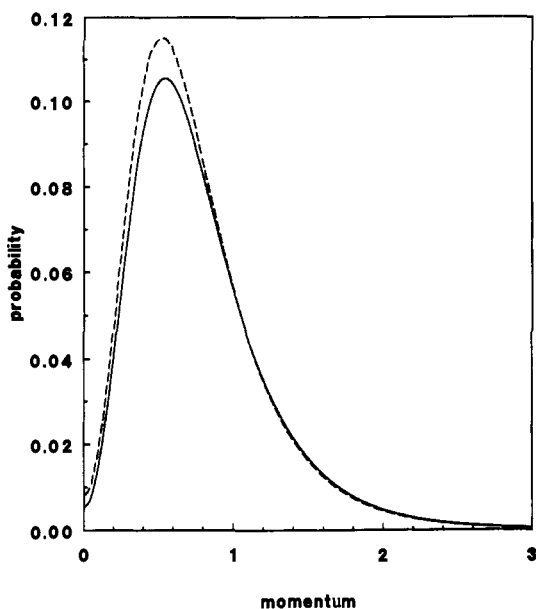
Figure 4. Spherically-averaged momentum density for the $3a_1$ Koopmans' (solid) and Dyson (dashed) orbitals of NH_3.
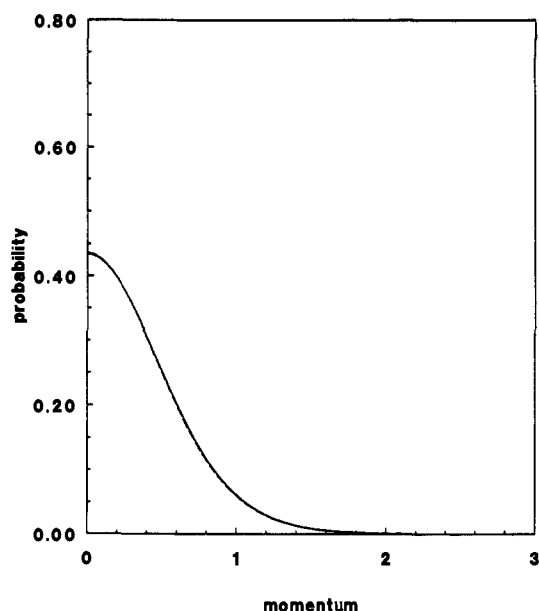
Figure 6. Spherically-averaged momentum density for the $2a_1$ orbital of NH_3.
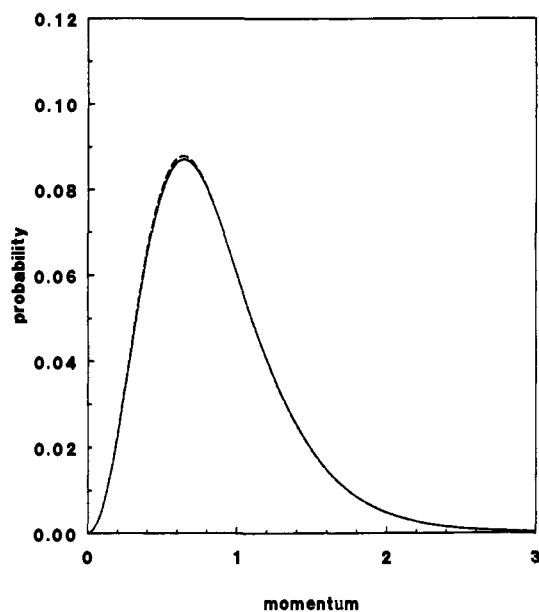
Figure 5. Spherically-averaged momentum density for the $1e$ Koopmans' (solid) and Dyson (dashed) orbitals of NH_3.
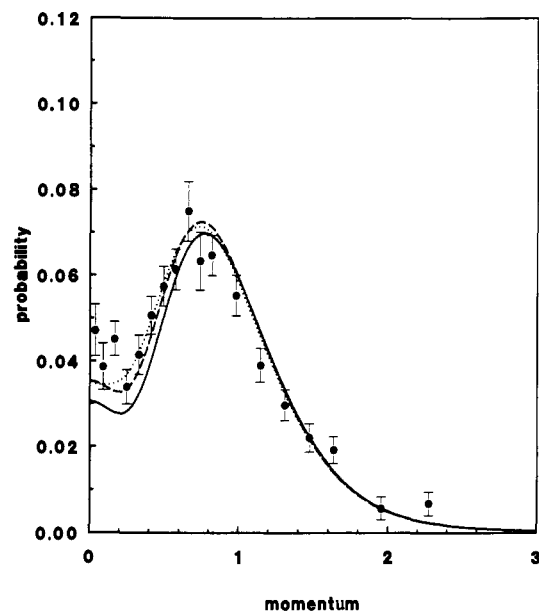
Figure 7. Spherically-averaged momentum density for the $7a'$ Koopmans' (solid) and Dyson (dashed) orbitals of CH_3NH_2. Also shown is the convoluted Dyson orbital (dotted) which should be compared with the experimental data taken from ref 4.

posed mainly of the 2s orbital of carbon combined in phase with the 1s orbitals of hydrogen. This gives a large value at zero momentum. These plots agree well with results reported in a previous publication.[16,17] Electron correlation is known to have very little effect on the results.

Figures 4–6 show the valence orbitals of ammonia. The $1e$ orbital has zero density at zero momentum and, like the t_2 orbital of CH_4, is composed mainly of p character at nitrogen and an e combination of s orbitals on hydrogen. The $2a_1$ orbital has a large value at zero momentum and consists mainly of an in-phase combination of 2s on nitrogen and 1s on hydrogen. It has some sp hybridization to give an effective hybrid pointing from nitrogen toward hydrogen. The $3a_1$ orbital has a very small value at zero

momentum. This orbital is mostly a p orbital on nitrogen. It has some 2s nitrogen character to form a hybrid pointing away from hydrogen. This forms a "back-side" bond with the hydrogens in which the hydrogen and nitrogen s character enter with opposite sign and tend to cancel in eq 10. Configuration interaction results are included for ammonia. Only the lone-pair orbital density is affected noticeably by electron correlation. Table II shows that S^2 is about 0.87, and this factor has not been included in the figure. The $2a_1$ orbital shape appears to be affected very little by correlation, but the small S^2 value in Table II indicates this primary hole is contributing to several satellite states.

Comparing the NH_3 results with those published recently by Bawagan et al.[18] shows excellent agreement. Because the experiment yields cross sections that are normalized relative to each other, but not normalized to any absolute scale, they normalized the $1e$ experimental profile at the maximum height to the best

---

(16) Clark, S. A. C.; Reddish, T. J.; Brion, C. E.; Davidson, E. R.; Frey, R. F. *Chem. Phys.* **1990**, *143*, 1.

(17) All of the previous collaborative work focused on comparison with EMS data. Because of finite resolution of the instrument, these previous publications showed theoretical results which have been folded with an estimated instrumental resolution to yield curves that could be directly compared with experiment. In the present publication, we show the true calculated momentum distribution of the molecule.

(18) Bawagan, A. O.; Muller-Fiedler, R.; Brion, C. E.; Davidson, E. R.; Boyle, C. M. *Chem. Phys.* **1988**, *120*, 335.
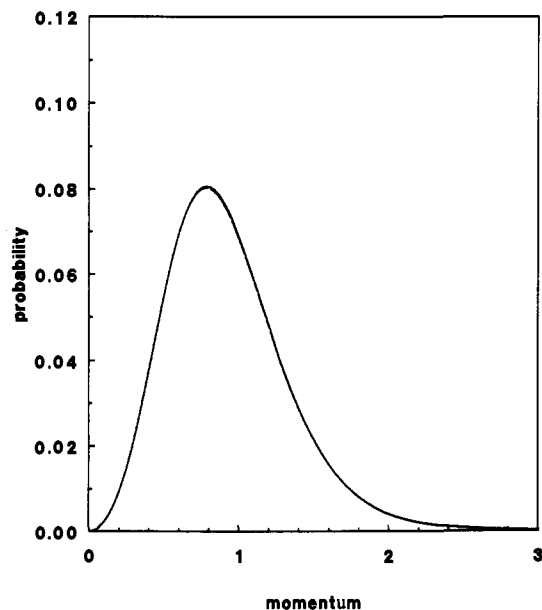
Figure 8. Spherically-averaged momentum density for the 2a″ Koopmans' (solid) and Dyson (dashed) orbitals of CH_3NH_2.
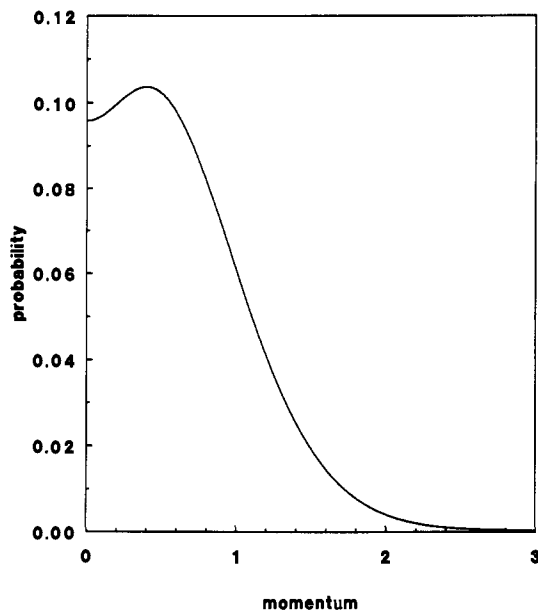
Figure 10. Spherically-averaged momentum density for the 5a′ Koopmans' orbitals of CH_3NH_2.
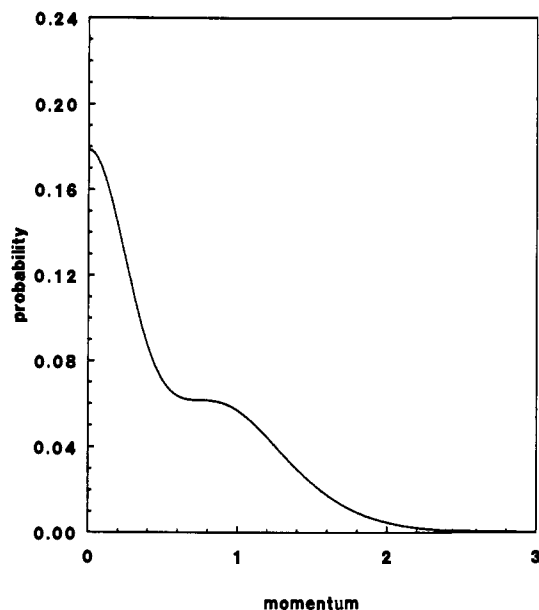
Figure 9. Spherically-averaged momentum density for the 6a′ Koopmans' orbitals of CH_3NH_2.
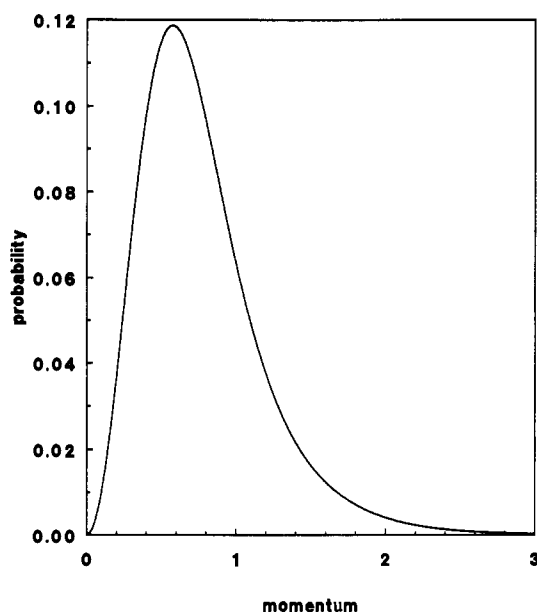
Figure 11. Spherically-averaged momentum density for the 1a″ Koopmans' orbitals of CH_3NH_2.

calculation and applied this same scaling factor (after adjusting for the 2-fold degeneracy of the e state) to the other valence orbitals. All momentum distributions at the CI level are found to agree well with the previous calculations. In the case of the $3a_1$ orbital, CI is needed to obtain agreement with experiment, while the Hartree–Fock distribution gives an orbital density 10% too low in the region near the peak (ignoring the S^2 factor).

Figures 7–13 show the valence orbitals for methylamine. As indicated by Figure 1, the HOMO 7a′ should correlate with the lone pair of ammonia. The 1a″ and 2a″ orbitals look like the t_2 orbital of methane and the e orbital of ammonia, respectively. The 3a′ to 6a′ orbitals are the four delocalized a′ bonding orbitals. The lowest of these has the s component from the atoms entering in phase and resembles the lowest valence orbital of CH_4 and NH_3. The other three a′ bonds have much smaller density at zero momentum because the s component enters with a variable sign from the different atoms. Like the lone-pair orbital, they have a large p component which gives a second maximum in the momentum density.

Tossell et al.[1] and Bawagan and Brion[2] also performed theoretical calculations on the HOMO of CH_3NH_2 but were unable

to obtain good agreement with the experimental profile. The STO-3G+G basis set Koopmans results gave the best line shape but predicted too great an intensity in the low momentum region. The 4-31G and 4-31G* distribution was much lower in intensity (70% lower at $p = 0$), shifted to higher momentum overall, and failed to predict the secondary maximum at zero momentum.

In order to compare our calculated result for the 7a′ orbital with the experimental data, we first folded our theoretical CI result with a function designed to simulate finite experimental resolution.[19] Because of the finite apertures in the experimental instrument, the resolution is somewhat reduced which leads to averaging of the data over a range of momenta. The experimental data were least-squares fit to the folded theory to determine the proportionality constant between orbital density (electrons per au^3 where the atomic unit of momentum is $\hbar/a_0$) and observed signal intensity. Figure 7 shows the folded CI result and the scaled

(19) This was done for us at the University of British Columbia by P. Duffy, using the method given in: Bawagan, A. O.; Brion, C. E. *Chem. Phys.* **1990**, *144*, 167. Duffy, P.; Casida, M. E.; Brion, C. E.; Chong, D. P. *Chem. Phys.* **1992**, in press.
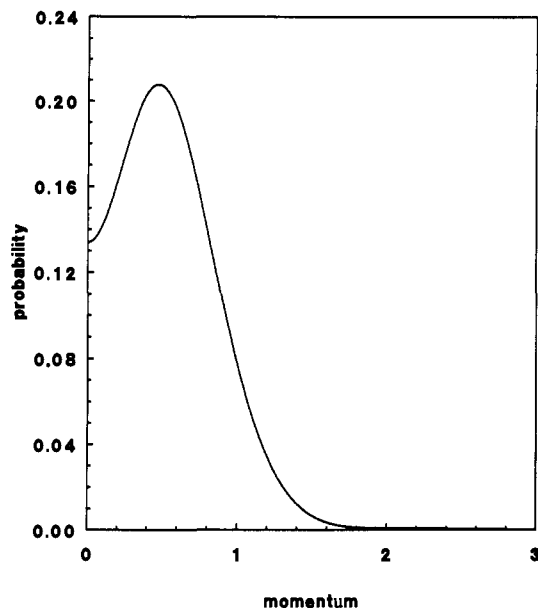
Figure 12. Spherically-averaged momentum density for the 4a′ Koopmans' orbitals of CH_3NH_2.
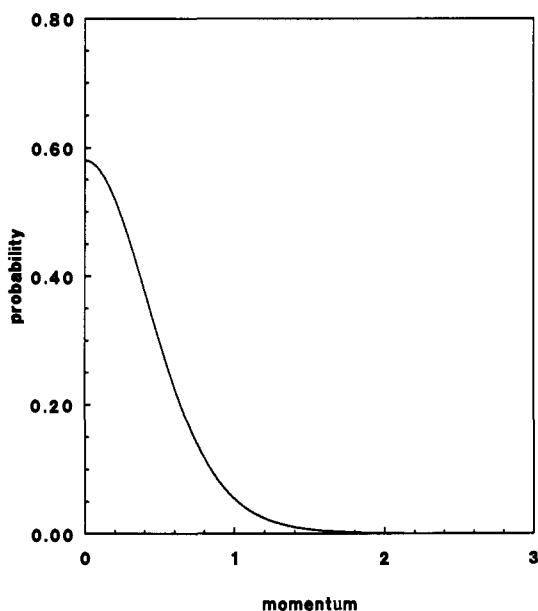
Figure 13. Spherically-averaged momentum density for the 3a′ Koopmans' orbitals of CH_3NH_2.

Table III. Charge Distribution Results (Mulliken Populations)

molecule		total	HOMO
NH_3	N	7.89	0.96
	H	0.70	0.01
CH_3NH_2	C	6.29	0.09
	H_1	0.87	0.09
	H_2	0.85	0.01
	H_3	0.85	0.01
	N	7.71	0.77
	H_4	0.72	0.01
	H_5	0.72	0.01
CH_4	C	6.63	0.56
	H	0.84	0.11
$CH_3NH_2^+$	C	6.39	
eclipse	H1	0.75	
	H2	0.73	
	H3	0.73	
	N	7.18	
	H4	0.60	
	H5	0.61	
NH_3^+	N	7.25	
	H	0.58	

experimental data points as well as the calculated true momentum distributions. The theory matches experiment quite well in the high-momentum region. In the very-low-momentum region the folded CI calculation falls shy of the error bars, and the rise near zero momentum is not predicted.

Bawagan and Brion also qualitatively determined that the methyl group was intrinsically electron withdrawing based on the trend in the HOMO momentum density in the sequence $NH_{3-n}(CH_3)_n$. They found, by experiment, that the amount of s character in this orbital (as measured by the density at zero momentum) continues to rise along this sequence. To investigate the validity of this conclusion more quantitatively, Mulliken population analyses were performed on NH_3, CH_3NH_2, and CH_4.

The HOMO electron distribution given in Table III clearly shows a shift of electrons away from nitrogen in going from ammonia to methylamine. Nearly 0.09 electron appears at both the carbon and hydrogen anti to the nitrogen lone-pair in the neutral molecule with a corresponding 0.19-electron loss at nitrogen compared to ammonia. Notice these HOMO populations are based on one electron. In the total molecular population shifts, these contributions will be doubled. These Mulliken populations

certainly agree with the experimental conclusion regarding the trend in the charge distribution in the HOMO. This HOMO orbital is antibonding between C and N as noted in ref 1 but CH bonding. Thus the CH character comes predominantly from delocalization of π_{CH} and n_N and not from admixing of π_{CH}^*.

Comparing the total nitrogen population in methylamine with ammonia shows that nitrogen has lost 0.17 electron, so one could say that carbon is electron withdrawing (relative to hydrogen) in agreement with Hehre and Pople.[4] At the same time the carbon in methylamine has lost 0.34 electron compared to methane, so one could equally say that nitrogen is electron withdrawing (relative to hydrogen). The same contradiction appears if one focuses instead on group charges. Then NH_2 has a charge of −0.30 in ammonia and −0.15 in methylamine so the methyl group seems to be electron withdrawing relative to hydrogen (but electron donating on an absolute scale). The charge on CH_3 is −0.16 in methane and +0.15 in methylamine so the amino group also seems to be electron withdrawing (on both a relative and absolute scale).

The contradiction arises because two hydrogens with a combined charge of 0.46 are lost in forming methylamine from ammonia and methane. This charge must be made up by a loss of 0.46 electron from the methyl and amino groups, with the result that both groups appear to lose electrons. Upon formation of methylamine, NH_2 loses 0.15 electron and CH_3 loses 0.31 accounting for the 0.46.

Methyl groups are often regarded as electron releasing compared to hydrogen because of the basicity of amines and stability of carbocations. In both of these examples it is found that positively charged molecules are energetically stabilized by adjacent methyl groups. Table III gives the populations for HNH_2^+ and $CH_3NH_2^+$ which allow a comparison of methyl with hydrogen in the cation. The NH_2 group has a charge of +0.58 in NH_3^+ and +0.61 in $CH_3NH_2^+$. In this case, the methyl group has little effect on the charge relative to hydrogen, but if anything it is still slightly electron withdrawing. Methylamine does have a lower ionization potential than ammonia in agreement with the shift in lone-pair orbital energy of the neutral molecule. This is probably best viewed as a destabilization of the lone-pair in the neutral by the methyl rather than a stabilization of the cation. The mixing between the CH bond orbital and the lone-pair stabilizes the lower-energy bond orbital but is antibonding with respect to the higher-energy lone-pair orbital.

Hehre and Pople[4] noted that the proton affinity for ammonia and methylamine calculated as an RHF/STO-3G energy difference favored methylamine in spite of the charge transfer being reversed from the expected result. Umeyama and Morokuma[5] explained this based on the greater polarizability of the HOMO of methylamine. We have repeated that calculation with the MP2/6-31G** wave function and find a proton affinity for ammonia of 220 kcal/mol and for methylamine of 230 kcal/mol

Table IV. Ammonia Radical Cation Hyperfine Parameters

atom		HF[a]	CI[a]	HF[b]	CI[b]	exp
		NH₃⁺ Ion Geometry				
		Isotropic Hyperfine Parameters (G)				
N		0	36.2	0	36.8	38
H		0	−28.8	0	−28.7	−28
		Anisotropic Hyperfine Parameters (G)				
N	x	−13.3	−16.6	−17.0	−16.6	−13
	y	−13.3	−16.6	−17.0	−16.6	−13
	z	26.6	33.1	34.0	33.2	26
H	x	−16.0	−20.3	−18.0	−20.3	−1.4
	y	−0.9	−4.6	−3.7	−4.7	0.7
	z	16.9	24.9	21.6	25.0	0.7
		NH₃ Neutral Geometry				
		Isotropic Hyperfine Parameters (G)				
N		41.5	75.9	60.1	76.9	
H		17.3	−8.0	14.4	−8.3	
		Anisotropic Hyperfine Parameters (G)				
N	x	−11.8	−14.5	−15.0	−14.5	
	y	−11.8	−14.5	−15.0	−14.5	
	z	23.6	29.0	30.0	29.0	
H	x	−14.6	−18.1	−15.9	−18.1	
	y	−2.5	−5.7	−5.2	−5.6	
	y	17.1	23.8	21.1	23.8	

[a] Calculation based on neutral molecule orbitals. [b] Calculation based on ion orbitals. [c] Reference 13.

Table V. Methylamine Hyperfine Parameters for the CH₃NH₂⁺ Geometry

atom		HF[a]	CI[a]	HF[b]	CI[b]	exp[c]
		Isotropic Hyperfine Parameters (G)				
C		0.0	−10.5	0.0	−9.1	
H₁		80.3	91.4	33.7	66.0	
H₂		17.8	19.7	7.1	14.2	
(H₁ + H₂ + H₃)/3		38.6	43.6	16.0	31.4	47
N		0.1	27.7	0.1	30.3	
H₄		0.0	−20.9	0.0	−21.7	−21
		Anisotropic Hyperfine Parameters (G)				
C	x	−3.8	−3.0	−2.7	−2.4	
	y	−0.5	−0.9	0.9	0.1	
	z	4.3	3.9	1.9	2.3	
H₁	x	−4.0	−3.7	−3.5	−3.4	
	y	−1.9	−1.6	−1.8	−1.5	
	z	5.9	5.3	5.3	4.9	
H₂	x	−2.5	−2.6	−2.5	−2.5	
	y	−1.6	−1.4	−2.2	−1.7	
	z	4.1	4.1	4.7	4.3	
N	x	−11.6	−14.8	−16.4	−15.8	−11
	y	−11.6	−14.7	−16.4	−15.8	−11
	z	23.2	29.4	32.7	31.6	22
H₄	x	−13.9	−17.6	−17.4	−18.8	
	y	−0.7	−3.4	−3.3	−3.8	
	z	14.6	21.0	20.7	22.6	

[a] Calculation based on neutral molecular orbitals. [b] Calculation based on ion orbitals. [c] Reference 5.

Table VI. Methylamine Hyperfine Parameters for the CH₃NH₂ Neutral Geometry

atom		HF[a]	CI[a]	HF[b]	CI[b]
		Isotropic Hyperfine Parameters (G)			
C		2.3	−8.2	2.7	−5.7
H₁		84.2	97.3	29.0	61.4
H₂		14.0	15.2	3.8	8.5
(H₁ + H₂ + H₃)/3		37.4	42.6	12.2	35.0
N		30.0	54.7	48.3	61.9
H₄		16.2	1.0	14.4	−0.9
		Anisotropic Hyperfine Parameters (G)			
C	x	−4.2	−3.3	−2.8	−2.5
	y	−1.9	−2.6	−1.7	−1.7
	z	6.1	6.0	4.5	4.2
H₁	x	−3.8	−3.3	−3.5	−2.8
	y	−2.5	−2.1	−1.8	−1.4
	z	6.2	5.3	5.3	4.2
H₂	x	−2.6	−2.7	−2.7	−2.5
	y	−1.9	−2.1	−2.2	−2.3
	z	4.5	4.8	4.9	4.8
N	x	−10.4	−13.0	−14.8	−14.3
	y	−10.4	−12.9	−14.8	−14.2
	z	20.8	−25.9	−29.6	−28.4
H₄	x	−12.3	−15.3	−15.5	−16.7
	y	−2.5	−4.8	−5.0	−5.3
	z	14.9	20.1	20.5	22.0

[a] Calculated using neutral molecule orbitals. [b] Calculated using ion orbitals.

(using MP2 optimized coordinates for all species).[20] The charge distribution in the protonated species shows that CH₃ is a slightly better electron donor, by an insignificant 0.01 electron, than hydrogen. So in both the cation and protonated molecule, methyl and hydrogen are equivalent donors, while in the parent form methyl is relatively electron withdrawing.

Isotropic and anisotropic coupling parameters were determined for ¹⁴NH₃⁺ and are listed in Table IV. Satisfactory agreement with the experimental values[21] was found for those parameters that are comparable. The isotropic (Fermi contact) parameters for NH₃⁺ are good, as are the nitrogen anisotropic values. The experimental anisotropic values for the hydrogens are obviously unreliable. These seem to have been averaged to zero by rotation of the ion in the matrix. This table illustrates the difficulty in learning about the HOMO from ESR Fermi contact data. The Hartree–Fock values using neutral molecule orbitals and geometry contain the interesting information. If these hydrogen values are divided by 1420 G, the value for a free hydrogen atom,[21] a value of 0.01 is obtained as the estimate of the HOMO orbital which is on hydrogen. This agrees well with Table III. The nitrogen result can be divided by 1811 G, the SCF value for the 2s orbital of a free nitrogen atom,[21] to obtain 0.02 as the nitrogen 2s population for one electron in the HOMO. Relaxation of the orbitals by doing the SCF calculation for the ion has only a small effect on the values. Configuration interaction, however, changes them markedly. Geometrical relaxation from the pyramidal neutral structure to the nearly planar radical cation structure causes the HOMO to become approximately a π orbital with a node through the nearby nuclei. The total isotropic contribution then comes from spin polarization effects in the CI. The spin density at the adjacent hydrogen can then be interpreted using the McConnell[22] relation as spin polarization of the NH bond caused by an unpaired electron in a π orbital on the adjacent nitrogen.

The anisotropic hyperfine interaction is easier to interpret. It is changed very little by orbital relaxation, geometric relaxation,

or CI. The nitrogen p component of the lone-pair orbital gives almost all the contribution, both at nitrogen and at hydrogen, in the SCF calculation at the NH₃⁺ geometry. The values given in this table are the eigenvalues of the tensor, so they are independent of the choice of axis system or molecular orientation. The x, y, z labels refer to the molecule fixed axis system in which the tensor is diagonal.

Tables V and VI give the hyperfine results for methylamine (based on ¹³C and ¹⁴N). Again, it is the SCF result in Table VI using the neutral molecule HOMO and geometry that carries the most interesting chemical information. Dividing the Fermi contact value for H₁ by the free atom value gives 0.06 for the fraction of the HOMO orbital that is on the hydrogen anti to the lone-pair. This method of obtaining populations weights the overlap population much less than does the Mulliken method so it tends to give smaller populations. The overlap population in the HOMO is

(20) The experimental values are 207 kcal/mol for NH₃ and 217 kcal/mol for CH₃NH₂. Aue, D. H.; Webb, H. M.; Bowers, M. T. *J. Am. Chem. Soc.* **1972**, *94*, 4726. Bowers, M. T.; Aue, D. H.; Webb, H. M.; McIver, R. T. *J. Am. Chem. Soc.* **1971**, *93*, 4313.
(21) Weltner, W. *Magnetic Atoms and Molecules*; Van Nostrand Reinhold: Berkshire, England, 1983.
(22) McConnell, H. M. *J. Chem. Phys.* **1956**, *24*, 764.
(23) Marcellus, D. H.; Davidson, E. R.; Kwiram, A. L. *Chem. Phys. Lett.* **1975**, *33*, 522.

negative for the N–C and N–H$_1$ interaction but positive for C–H$_1$ in agreement with the idea that the HOMO is an antibonding mixture of the CH bond and the N lone-pair. Orbital relaxation to the ion orbitals greatly reduces this unpaired density. Geometrical relaxation to the ion conformation has little effect on this interaction. Unfortunately, spin polarization effects represented by the CI are large, so the experimental Fermi contact value gives little information about the HOMO orbital.

The anisotropic hyperfine tensor is much less affected by relaxation and polarization. The values at C and H$_1$ can be regarded as through space interaction of these nuclei with an unpaired electron in the nitrogen lone-pair orbital.

Experimental data[5] are also available for the deuterated compound CH$_2$DNH$_2$$^+$. Without deuteration the CH$_3$ group appears to be freely rotating and all methyl protons are equivalent. With one deuterium present the Fermi contact results (scaled by g_H/g_D to make comparison easier) are 18 G for D and 61 G for H. These average to the same 47 G found for CH$_3$. This indicates that H has a preference compared to D for occupying the anti position in the ion.

For comparison, we have calculated the Fermi contact for the eclipsed form of the ion. The CI calculation with ion orbitals gives –0.3 G for the H with its CH bond in the nodal plane of the singly occupied orbital and 46.7 for the other two. The average of these is 31.0 G which is close to the 31.4 G average calculated in the staggered conformation.

This is in agreement with past theory for the ethyl radical which suggested that $a_{iso}(H)$ could be fit by[23]

$$a_{iso}(H) = c + b \cos^2 (\chi) \qquad (11)$$

where χ is the dihedral angle between the CH bond and the π orbital of CH$_2$. This model assumes that the ethyl CH$_2$ group is planar and the only geometrical variable is χ. The average of this for three hydrogens spaced at equal angles is $c + \frac{1}{2}b$ independent of χ. A recent calculation on ethyl[3] gave the average as 19.7 G in the staggered form and 19.2 G in the eclipsed form (this reference labeled the two forms opposite to the notation used here). It is interesting to note that the spin densities indicate greater hyperconjugation in methylamine radical cation than in ethyl.

The calculation indicates that "c" is small we will neglect it. In that case the experimental data suggest that "b" is 94 G. The energy for internal rotation shows a preference for the staggered form. In the three possible positions of the staggered conformation, the value of $a(D)$ would be 94, 23.5, and 23.5. All of these values are larger than the observed value for $a(D)$. Clearly D has a low probability of being in the anti position. If the two protons were oscillating between the anti position, then D would remain inside of the ±30° range around the nodal plane of the nitrogen π orbital where the $a(D)$ value is less than 23.5 G. This indicates that the force constant for stretching the anti CH bond is less than that for stretching the others. This is consistent with hyperconjugation leading to a partial removal of the spin-down CH bonding electron.

To confirm this interpretation, we calculated the vibrational frequencies from the UHF energy with the 6-31G* basis at the UHF minimum. The methyl CH$_3$ bending mode of e symmetry is split by the NH$_2$ group into an a′ mode (large anti H motion) and an a″ mode (no anti H motion). Similarly, the a and e CH stretch modes become two a′ modes (large anti H motion) and an a″ mode (no anti H motion). In both cases, the a′ part of the e mode has lower frequency than the a″ part, indicating a weakening of anti CH bend and stretch force constants.

With one deuterium on carbon, the zero-point energy is predicted to be 29 cm^{-1} (42 K) lower with a hydrogen in the anti position compared to the deuterium. At liquid helium temperature, this is enough energy difference to keep deuterium out of the anti position. The calculation shows that 10 cm^{-1} of this preference comes from stretching modes and the rest from bending modes.

Conclusion

The calculations are in reasonable agreement with the experimental data on methylamine and its cation. The EMS data give an indication that the HOMO of the neutral molecule is delocalized onto the methyl. While it is true that the methyl group is electron withdrawing relative to hydrogen, that conclusion does not follow from the EMS data alone since electron transfer is partly a σ bond electronegativity effect.

The EPR data are more difficult to interpret. Because of geometrical relaxation in the ion, the cation spin distribution around nitrogen is fairly different from the HOMO distribution in the neutral molecule. Additionally, spin polarization renders the Fermi contact part of the hyperfine interaction difficult to interpret. The anisotropic part, however, is more easily interpreted as it is dominated by the HOMO contribution and is little changed from the HOMO of the neutral.